sustainability

MDPI

Article

A Data-Driven Framework for Health-Promoting Trail Network Planning Using Multi-Source Geospatial Data: Evidence from Qingdao, China

Yang Zhao [1,*], Linzhen Wei [1], Deming Liu [2], Huaiyu Yang [1], Chenyang Shi [1], Ledan Sun [1] and Lukai Wang [1]

[1] College of Architecture and Urban Planning, Qingdao University of Technology, Qingdao 266033, China
[2] School of Architecture and Design, Harbin Institute of Technology, Harbin 150001, China; liudeming@hit.edu.cn
* Correspondence: zhaoy@qut.edu.cn; Tel.: +86-176-8551-7561

Abstract

Health-promoting trail (HPT) networks can provide spatial support for walking-based physical activity and healthy city development. Yet existing planning approaches often address environmental suitability or route optimization without fully integrating spatial continuity, network generation, and service potential. This study develops a data-driven framework for HPT network planning using multi-source spatial data (MSSD), with the eastern urban area of Qingdao, China, as a case study. Previously published choice-based conjoint (CBC) preference estimates were used to weight eight environmental indicators in a geographic information system (GIS) to calculate a fitness suitability index (FSI). Connection nodes were linked by routes minimizing the length-weighted inverse FSI, and urban spaces with high continuity potential were incorporated as planning corridors. The generated network's service potential was evaluated through Euclidean proximity coverage of residential locations and estimated population, together with network length within residential proximity buffers. The spatial assessment identified limited provision of long continuous walking segments in the existing walking network. The proposed integration identified opportunities for longer continuous walking corridors and extensive potential residential coverage. By linking preference-informed assessment, geospatial network generation, and service potential evaluation, the framework supports sustainable urban planning by identifying opportunities to coordinate existing urban spatial resources for health-promoting walking infrastructure.

Keywords: choice-based conjoint analysis; geospatial analysis; walking-based physical activity; fitness suitability; route generation; spatial continuity; Euclidean proximity coverage

Check for updates

Academic Editor: Kalliopi Kyriakou

Received: 27 September 2026
Revised: 1 November 2026
Accepted: 2 November 2026
Published: 5 November 2026

Copyright: © 2026 by the authors. Licensee MDPI, Basel, Switzerland. This article is an open access article distributed under the terms and conditions of the Creative Commons Attribution (CC BY) license.

1. Introduction

Physical inactivity has become a major contributor to chronic diseases and public health risks, making the promotion of daily physical activity (PA) through built-environment interventions an important issue in healthy city development [1,2]. Walking, as an accessible form of PA that can be readily integrated into daily life, is associated with health benefits [3]. Higher daily step counts have been associated with lower risks of chronic conditions such as type 2 diabetes and cardiovascular disease [4]. In this context, linear public spaces such as greenways and walking trails have become increasingly important for supporting walking-based PA. By connecting places of daily activity while providing continuous, safe, and comfortable walking environments, these spaces can facilitate activities such as brisk

and fitness walking and have consequently become an important component of healthy city development and public fitness infrastructure [5].

Planning walking environments is relevant to urban sustainability through the provision of opportunities for daily PA and the coordinated use of existing urban spatial resources. Health-promoting trail (HPT) planning thus relates to the United Nations Sustainable Development Goals (SDGs), particularly SDG 3 on health and well-being and SDG 11 on sustainable cities, including Target 11.7 concerning access to green and public spaces [6].

Previous studies have extensively examined built-environment factors associated with walking behavior and trail use, including land use, street environments, landscape vegetation, traffic safety, accessibility, and public facility provision [7–9]. Specific environmental attributes, such as street gradient, pavement quality, trail width, greenery, safety facilities, and destination accessibility, have been shown to influence individuals' route choices, frequency of trail use, and levels of PA [7,9–11]. Beyond these attributes, path continuity represents an important environmental characteristic for sustained walking-based exercise. Longer uninterrupted routes can provide spatial conditions that support sustained walking and help reduce interruptions that may disrupt walking intensity [12]. However, existing studies have predominantly focused on general walking behavior or recreational activities, with comparatively limited attention to the continuity required for sustained walking-based exercise [9,12]. In particular, an integrated analytical framework that combines fitness suitability assessment with the spatial requirements of continuous walking remains lacking. Consequently, translating residents' actual preferences for walking-based fitness environments into quantifiable environmental assessments, while identifying spatial resources with the potential to support continuous walking, remains an important challenge for the planning of health-oriented walking environments.

In terms of planning methods, suitability assessment, network analysis, and least-cost path approaches have been widely applied to greenway and trail routing, often in combination with geographic information system (GIS) techniques to identify suitable walking spaces [13,14]. In recent years, multi-source spatial data (MSSD), including points of interest (POIs), remote sensing imagery, road network data, and population data, have expanded the data foundation for urban-scale walking-environment assessment and health-oriented walking-space planning [15,16]. In this study, an HPT is defined as a linear public space planned to support regular walking-based PA by providing a suitable, continuous, safe, and accessible walking environment; an HPT network therefore refers to an interconnected system of such spaces organized to serve residents' daily activity needs.

The present study builds on three earlier investigations of walking-based fitness environments in Qingdao. A social-network study identified environmental demands from user-generated descriptions of walking routes [17], providing a conceptual basis for understanding fitness suitability. A subsequent choice-based conjoint (CBC) study quantified environmental preferences and estimated attribute-level utilities and relative importance scores [18]. A continuity-oriented planning study identified four types of high-continuity spaces and connected them with existing walking spaces and metro stations through continuity-based least-cost routing [19]. That study also evaluated the resulting network in terms of continuity, proximity coverage, environmental comfort, and spatial composition.

These studies provide complementary foundations, but the CBC preference estimates were not incorporated into the continuity-based route-selection model. In the earlier planning study [19], continuity determined routing impedance, whereas slope and vegetation were primarily used to evaluate the selected routes. The remaining methodological task is therefore to translate the previously identified environmental preferences into a multi-indicator spatial assessment and use that assessment to guide network generation, while retaining continuity as an explicit consideration in network organization.

This study addresses this task through an integrated planning framework applied to the eastern urban area of Qingdao. The previously published CBC importance scores [18] are reused as weighting inputs for an eight-indicator GIS-based fitness suitability assessment. The resulting fitness suitability index (FSI) informs route generation around residential, workplace, public transport, and open-space nodes. The high-continuity space typology established in the earlier planning study [19] is retained and incorporated into this broader planning process. The generated network is subsequently evaluated for its spatial service coverage and residential proximity. Accordingly, this study addresses three research questions:

(1) How can previously established environmental preference evidence be operationalized to assess the spatial distribution of fitness suitability across the walking network?
(2) How can fitness suitability, daily activity nodes, and high-continuity spatial resources be combined to generate an HPT network?
(3) What spatial service coverage and residential proximity does the generated network provide?

The contribution lies in linking previously separate preference and continuity research within a multi-indicator, activity-node-based planning workflow. The CBC survey and the four-type continuity-space classification are inherited foundations; their integration into the spatial assessment and network-generation process constitutes the methodological extension examined here.

Section 2 presents the data, indicator assessment, network-generation procedures, and evaluation methods. Section 3 reports the spatial assessments, generated scenarios, and proximity comparisons. Section 4 discusses planning implications and limitations, and Section 5 summarizes the conclusions.

2. Materials and Methods

2.1. Planning Framework

This study develops a data-driven planning framework for generating HPT networks using MSSD. Oriented toward residents' needs for walking-based fitness activities, the framework integrates multiple sources of data on behavioral preferences, the urban built environment, and spatial resources. It establishes an integrated workflow comprising three sequential components: fitness suitability assessment, HPT network generation, and service potential evaluation, thereby extending HPT planning from the identification of suitable routes toward network-based planning.

The framework consists of three interconnected modules. The fitness suitability assessment module evaluates the extent to which urban road environments support walking-based fitness activities and identifies suitable road spaces as the basis for subsequent network generation. The HPT network generation module organizes these road spaces around residents' daily activity nodes and integrates urban spaces with high continuity potential to generate an HPT network that considers both fitness suitability and spatial continuity. Finally, the service potential evaluation module assesses residential and population proximity to the generated network and the network length within residential proximity buffers. Together, these three modules constitute the proposed data-driven planning framework for HPT network generation (Figure 1).

2.2. Study Area

Since Qingdao launched its Healthy City initiative in 2019, improving public fitness infrastructure to meet residents' growing demand for PA has become an important component of urban development. In recent years, the city has also promoted the development of an "8-min fitness circle" to improve residents' access to fitness facilities and spaces [20]. As a typical coastal city in China, Qingdao has a mild climate and abundant landscape resources

that provide favorable conditions for outdoor walking-based fitness activities. However, spaces supporting such activities remain spatially fragmented across the city. Apart from Shinan District, where walking spaces are relatively concentrated along the coast and centered on the Qingdao Coastal Walkway, most existing facilities are distributed around urban parks, public squares, green spaces, and mountainous scenic areas. These spaces lack sufficient linear connections that can function as HPTs, resulting in limited network integration and an insufficient citywide trail network to support outdoor walking-based fitness activities.

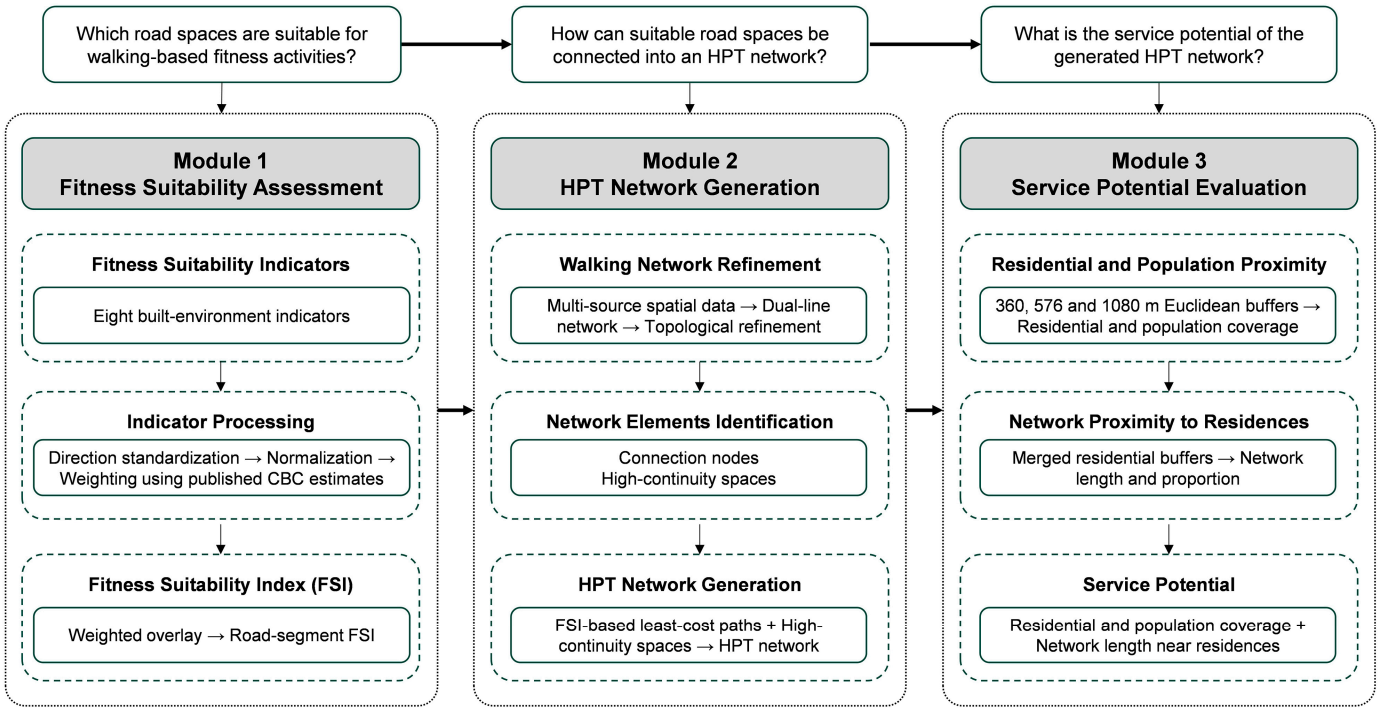


Figure 1. Planning framework for health-promoting trail (HPT) network generation. The figure uses the abbreviation for choice-based conjoint (CBC).

Qingdao comprises seven urban districts and administers three county-level cities. The eastern urban area, which forms part of Qingdao's main urban area, encompasses Shinan, Shibei, Licang, and Laoshan districts and serves as a major administrative, cultural, educational, tourism, and residential center of the city. Although it accounts for only 5.25% of Qingdao's total land area, it accommodates 28.03% of the city's permanent resident population, with population densities exceeding 1000 persons/km^2 in all four districts [21,22]. This concentration of population implies substantial demand for accessible spaces supporting outdoor walking-based fitness activities. Meanwhile, as a densely developed central urban area with a relatively mature built environment, opportunities for constructing entirely new trail infrastructure are constrained. HPT planning therefore requires the systematic assessment of existing walking environments and the identification and integration of suitable linear spaces within the existing urban fabric. These characteristics make the eastern urban area an appropriate case for applying and examining the proposed planning framework (Figure 2).

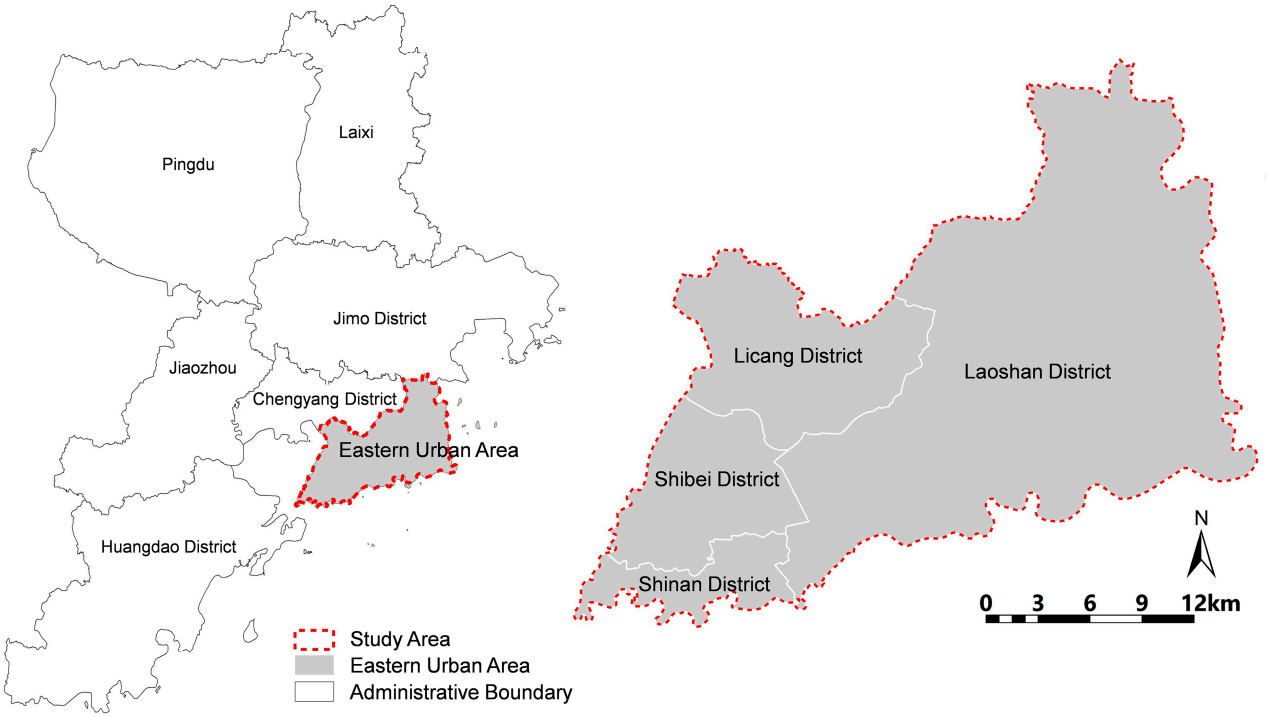


Figure 2. Location of the study area.

2.3. Fitness Suitability Assessment Indicators

2.3.1. Theoretical Basis and Indicator Selection

Drawing on the relevant literature and the environmental demands identified in the authors' previous social-network study in Qingdao [17], this study defines fitness suitability as the extent to which the built environment provides supportive conditions for walking-based fitness activities. These conditions include continuity, safety, comfort, and supporting facilities [7,17]. Reference [17] is used as a conceptual and empirical literature source; its original social-network records are not incorporated into the dataset analyzed in the present study.

Evidence from exercise and health research indicates that the health effects of walking are closely related to PA characteristics such as exercise intensity and duration, while maintaining these characteristics during walking also depends on the continuity of walking activity [12,23]. These characteristics are influenced not only by individual physical conditions but also by features of the built environment [7]. A supportive walking environment can reduce environmental barriers and pedestrian–vehicle conflicts, helping walkers maintain a stable pace, appropriate exercise intensity, and sufficient duration [7,12]. Accordingly, this study focuses on meso- and micro-scale built-environment characteristics that may affect the experience of walking-based fitness activities, including trail width, surface gradient, path continuity, supporting facilities, traffic interference, nighttime lighting, and the natural environment [7,17,24]. Together, these characteristics influence the safety, comfort, continuity, and convenience of walking and therefore provide the environmental basis for assessing fitness suitability.

The eight-indicator assessment system was developed by operationalizing the environmental attributes examined in the previous CBC study [18], with reference to the above conceptual framework and the availability of city-scale spatial data (Table 1). The indicators represent spatially measurable dimensions related to the original survey attributes. Some rely on proxy variables and therefore should not be interpreted as direct equivalents of the conditions described in the CBC choice tasks. The indicator quantification procedures and integrated fitness suitability assessment are described in Section 2.5.

Pavement material, surface evenness, and maintenance condition can also influence walking comfort and safety [9,17,25]. These characteristics were not included in the inherited CBC attribute set, and consistent segment-level data describing them were unavailable for the city-scale assessment. Their exclusion reflects the scope of the available preference evidence and spatial data, rather than an assumption that they are unimportant or uniform across the study area. The resulting indicator system is therefore intended for preliminary network planning; pavement and maintenance conditions should be checked during local route assessment and implementation.

Table 1. Fitness suitability assessment indicators and their descriptions.

Indicator	Description
Facility mix	Reflects the diversity of supporting facilities available in the walking environment. A greater facility mix can better support rest, refreshment, and other service needs during walking-based fitness activities, thereby improving convenience and comfort.
Slope	Reflects the influence of road slope on walking pace and physical exertion. Steeper slopes increase the energetic demands of walking and may therefore reduce fitness suitability, particularly for individuals with lower physical capacity [26].
Roadside space availability	Reflects the availability of space along roads for accommodating walking paths and supporting facilities. Greater roadside space availability provides more favorable spatial conditions for safe and comfortable walking-based fitness activities.
Path continuity	Reflects the extent to which the walking environment provides continuous and uninterrupted spatial support for sustained walking. Greater path continuity helps walkers maintain a stable pace and supports sustained walking-based fitness activities.
Crowding	Reflects the degree of crowding in the walking environment. Higher levels of crowding may interfere with walking movement and reduce the comfort of walking-based fitness activities [27].
Traffic flow impact	Reflects the degree of interference from motorized traffic in the walking environment. Greater traffic interference may affect walkers' movement and reduce the safety and comfort of walking-based fitness activities [28].
Nighttime light intensity	Reflects nighttime lighting conditions in the walking environment. Adequate nighttime lighting can improve perceived walking safety and support walking-based fitness activities during evening hours.
Vegetation coverage	Reflects the extent of vegetation in the walking environment. Greater vegetation coverage can improve natural and landscape qualities and thermal comfort, thereby enhancing the experience of walking-based fitness activities.

2.3.2. Previously Published CBC Evidence and Its Use in Indicator Weighting

The preference evidence was obtained from the earlier CBC investigation in Qingdao [18]. The weighting results used here are based on 442 respondents, as verified against the respondent-level hierarchical Bayes (HB) outputs. No new CBC survey was conducted. The original study combined online recruitment through walking groups with supplementary face-to-face fieldwork [18]. Within the 442-person analysis sample, 59.73% were male and 40.27% were female. Respondents aged 46–59 years constituted the largest age group (30.09%), whereas those aged 60 years or above accounted for 19.91%. Employees and students accounted for 45.93% and 35.97%, respectively. Additional sample characteristics are reported in Table S1.

The experiment included eight attributes, each with three qualitative levels. Their correspondence with the GIS indicators is described in Section 2.5.1, and a choice-task example is provided in Table S2. As reported in the original study [18], Lighthouse Studio 9.11.0 was used to generate 100 questionnaire versions using the balanced overlap method. Each version contained 10 randomized choice tasks and two fixed tasks, with two alternatives per task. The archived HB settings confirm that the two fixed tasks were excluded from estimation. Attributes were estimated as categorical part-worths, with 10,000 initial iterations before using results and 10,000 draws used for each respondent.

Under the random utility framework [29,30], the utility of alternative a for respondent r is expressed as:

$$U_{ra} = \sum_{i=1}^{n} \sum_{j=1}^{m_i} u_{rij} x_{aij} + \varepsilon_{ra} \quad (1)$$

where $n = 8$, $m_i = 3$, u_{rij} is the estimated part-worth utility of level j of attribute i for respondent r, x_{aij} indicates whether that level is present in alternative a, and ε_{ra} represents the unobserved utility component.

Attribute importance was calculated separately for each respondent from the range of part-worth utilities:

$$C_{ri} = max_j(u_{rij}) - min_j(u_{rij}) \quad (2)$$

The individual percentage importance and the mean weight used in the GIS assessment were then calculated as:

$$p_{ri} = 100 \frac{C_{ri}}{\sum_{k=1}^{n} C_{rk}}, \quad w_i = \frac{1}{100N} \sum_{r=1}^{N} p_{ri}, \quad N = 442 \quad (3)$$

Thus, importance scores were calculated at the individual level and subsequently averaged, rather than calculated from average utilities. Approximate 95% confidence intervals for mean percentage importance were calculated as $\overline{p}_i \pm \frac{1.96 s_i}{\sqrt{N}}$, where $\overline{p}_i$ and s_i are the sample mean and sample standard deviation of individual percentage importance, respectively. These intervals quantify uncertainty in the estimated mean importance scores, whereas the sample standard deviations describe variability among respondents. They are not HB posterior credible intervals. Weights were rounded to seven decimal places for the GIS calculation.

The original study also reported a preliminary test in which 30 participants completed the questionnaire twice within one week; 26 made consistent choices on the two fixed tasks, corresponding to 86.7% agreement [18]. This result is reported as a preliminary reliability check from the earlier investigation, rather than as a repeated assessment of the entire analysis sample.

2.4. Multi-Source Spatial Data

2.4.1. Data Acquisition and Preprocessing

To quantify the fitness suitability assessment indicators, MSSD were integrated to establish the database used in this study (Table 2) [15]. Given the different update cycles of the datasets, data from nearby years were used where available. For fundamental datasets with relatively long update cycles and authoritative official sources, such as census data, the most recently released official statistics were used. Together, these datasets provide the basis for quantifying built-environment characteristics and calculating the fitness suitability assessment indicators.

Table 2. Multi-source spatial datasets and their applications in the planning framework.

Dataset	Data Type/Spatial Resolution	Data Source	Year/Period	Main Application
Road network data	Vector data (line)	OSM	April 2025 update	roadside space availability; path continuity; traffic flow impact
POI data	Vector data (point)	AMAP Open Platform API	2025	Facility mix; connection node extraction
Population data	Statistical data	Seventh National Population Census Bulletin	2020	Service potential evaluation (Euclidean proximity coverage)
DEM data	Raster data, 30 m	Copernicus DEM GLO-30	Downloaded in 2025 *	Slope
Nighttime light data	Raster data, 500 m	NOAA VIIRS Annual Nighttime Light Dataset	2024	Nighttime light intensity
Baidu heatmap data	Raster data	Baidu Maps	8 April 2025 (Tuesday) and 12 April 2025 (Saturday); hourly, 05:00–23:00; 38 observations in total	Crowding
NDVI data	Raster data, 30 m	Resource and Environmental Science Data Platform	2024	Vegetation coverage
High-continuity space data	Vector data (line/polygon)	OSM	April 2025 update	Identification and integration of high-continuity spaces

*: The main underlying observations of Copernicus DEM date from 2011 to 2015; 2025 indicates the download year. Note: Abbreviations used in this table are OpenStreetMap (OSM), point of interest (POI), application programming interface (API), digital elevation model (DEM), National Oceanic and Atmospheric Administration (NOAA), Visible Infrared Imaging Radiometer Suite (VIIRS), and normalized difference vegetation index (NDVI).

Before indicator calculation, the datasets were preprocessed in ArcMap 10.2 to ensure spatial consistency and analytical accuracy. Vector datasets, including OpenStreetMap (OSM) and POI data, were cleaned to remove irrelevant and duplicate records and trans-

formed to WGS 84/UTM zone 51N (EPSG:32651). This projected coordinate system, with metres as its linear unit, was used for distance, length, and buffer calculations. The data were then clipped to the study area, manually checked, and supplemented with missing roads and pedestrian paths to improve the completeness of the base walking network. Raster data, such as digital elevation model (DEM) and normalized difference vegetation index (NDVI) data, were processed through coordinate transformation, spatial clipping, resampling, and outlier treatment as appropriate. The preprocessed datasets were subsequently integrated according to their spatial characteristics and the requirements of indicator quantification, providing a harmonized spatial database for the subsequent fitness suitability assessment, HPT network generation, and service potential evaluation.

2.4.2. Walking Network Refinement

Previous studies commonly represent pedestrian movement using street networks, in which road centerlines are used as proxies for walkable paths [31]. Although this representation is generally adequate for conventional transportation network analysis, it cannot accurately capture the continuity of walking spaces on both sides of a road [31,32]. This limitation is particularly evident at T-intersections with staggered junctions and in areas with grade-separated pedestrian crossings, where a single-line network cannot distinguish the continuity relationships between walking spaces on opposite sides of the road. Consequently, actually connected walking paths may be incorrectly identified as discontinuous, potentially biasing the measurement of path continuity.

To improve the accuracy of path continuity assessment, the conventional single-line network was refined into a topology-enhanced dual-line walking network. Road centerlines were converted into two parallel lines representing the walking spaces on either side of each road, with corresponding topological relationships established according to actual road configurations, allowing the two sides to be independently represented in network analysis (Figure 3). Where at-grade pedestrian crossings were available, topological connections were established according to actual crossing conditions. For grade-separated pedestrian facilities, such as pedestrian overpasses and underpasses, cross-road topological connections were established based on their actual spatial connections. Where no pedestrian crossing was available, walking paths separated by roads were retained as topologically disconnected.

The refined network retains the spatial structure of the original road network while more accurately representing the continuity of walking spaces on both sides of roads and the effects of different pedestrian crossing facilities on continuous pedestrian movement. Topological connectivity indicates whether movement between segments is possible; it does not establish uninterrupted walking. Continuity was assessed separately using the rules described in Section 2.5.1.

2.5. Indicator Quantification and Fitness Suitability Assessment

2.5.1. Indicator Quantification

Based on the assessment indicator system established above, the eight fitness suitability indicators were quantified using three GIS-based approaches: spatial analysis, topological analysis, and raster analysis (Table 3).

According to their directional effects on fitness suitability, environmental characteristics that support walking-based fitness activities were defined as positive indicators, including facility mix, roadside space availability, path continuity, nighttime light intensity, and vegetation coverage. In contrast, environmental characteristics that may hinder such activities were defined as negative indicators, including slope, crowding, and traffic flow impact. To ensure a consistent evaluation direction across all indicators, their directions were aligned and the values were standardized before the integrated fitness suitability assessment.

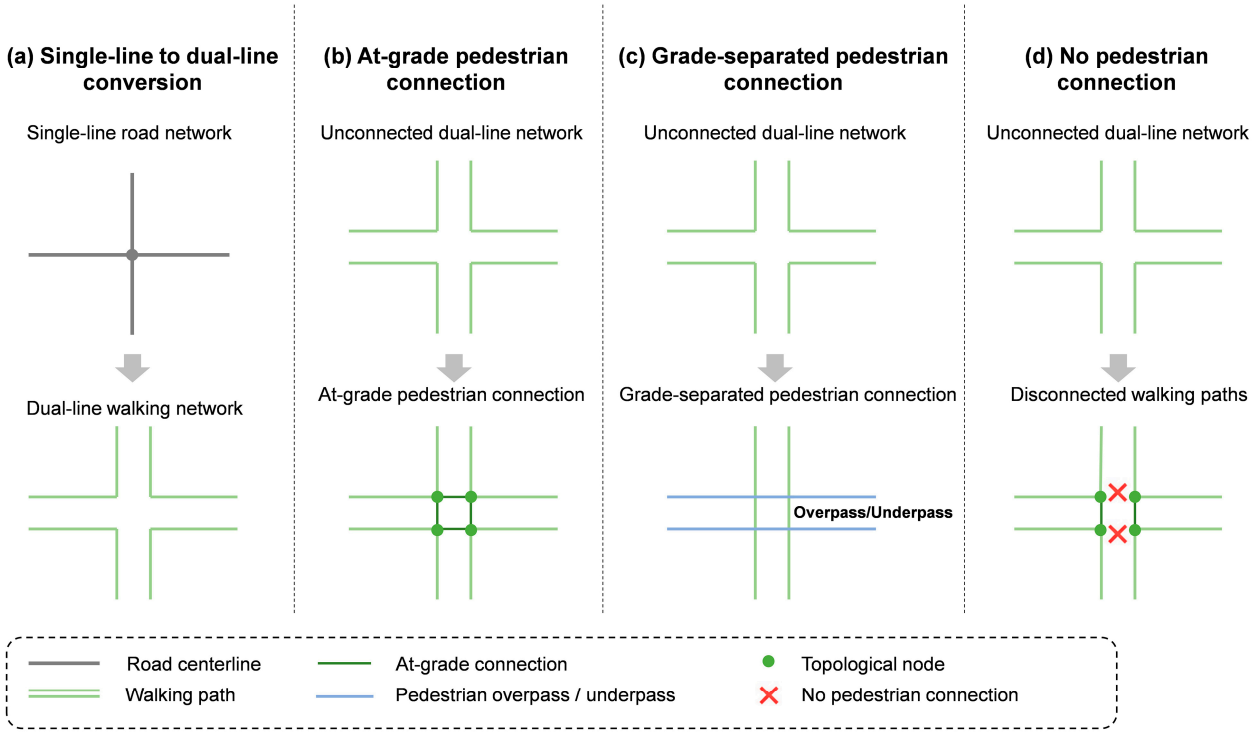


Figure 3. Schematic illustration of walking network refinement and topological connection rules.

Table 3. Correspondence between CBC attributes and geographic information system (GIS) indicators used in the fitness suitability assessment.

GIS Indicator	Corresponding CBC Attribute and Levels	Direction	Spatial Measurement
Facility mix	Supporting facilities: Level 1: No relevant supporting facilities. Level 2: A small number of relevant supporting facilities, with limited variety. Level 3: A large number of relevant supporting facilities, with diverse types.	+	Shannon entropy of five POI categories
Slope	Path slope: Level 1: Flat, without obvious changes in elevation. Level 2: Gentle slope, with slight changes in elevation. Level 3: Steep slope, with obvious changes in elevation.	−	Mean raster value
Roadside space availability	Walking width: Level 1: Narrow, with limited effective passage width. Level 2: Medium, with moderate effective passage width. Level 3: Wide, with ample effective passage width.	+	Road type and hierarchy as proxies
Path continuity	Path interruptions: Level 1: No interruptions, with good continuity. Level 2: Few interruptions, with moderate continuity. Level 3: Many interruptions, with poor continuity.	+	Continuous path length

Table 3. *Cont.*

GIS Indicator	Corresponding CBC Attribute and Levels	Direction	Spatial Measurement
Crowding	Pedestrian flow and crowding: Level 1: Low pedestrian flow, without crowding. Level 2: Higher pedestrian flow, with some crowding. Level 3: High pedestrian flow, with substantial crowding.	−	Mean raster value
Traffic flow impact	Motor-traffic interference: Level 1: No motor-traffic interference. Level 2: Low motor-traffic interference. Level 3: High motor-traffic interference.	−	Length-weighted sum of road speed limits within each grid cell
Nighttime light intensity	Light and lighting conditions: Level 1: Dim conditions, without artificial lighting. Level 2: Moderate light conditions, with some artificial lighting. Level 3: Bright conditions, with extensive artificial lighting.	+	Mean raster value
Vegetation coverage	Vegetation and visible greenery: Level 1: No vegetation or visible greenery. Level 2: Limited vegetation and visible greenery. Level 3: Abundant vegetation and visible greenery.	+	Mean raster value

Spatial analysis was used to quantify facility mix and traffic flow impact within a 500 m × 500 m fishnet grid, providing a neighborhood-scale representation of environmental conditions [33]. Facility mix was calculated using Shannon entropy for five AMAP mid-level POI categories: Sports Stadium, Recreation Place, Park & Square, Tourist Attraction Related, and Public Toilet:

$$H_g = -\sum_{i=1}^{5} p_{ig} \ln p_{ig}, \quad p_{ig} = \frac{N_{ig}}{\sum_{i=1}^{5} N_{ig}} \tag{4}$$

where H_g is facility mix in grid cell g, N_{ig} is the number of POIs in category i within that cell, and p_{ig} is the corresponding proportion. Terms with $p_{ig} = 0$ were treated as zero, and cells containing no POIs from these categories were assigned $H_g = 0$. Traffic flow impact was calculated as:

$$T_g = \sum_{j=1}^{m_g} v_j l_{jg} \tag{5}$$

where T_g is traffic flow impact in grid cell g, m_g is the number of road segments within the cell, v_j is the speed limit of road segment j, and l_{jg} is its length within the cell. The sum was not divided by total road length or grid-cell area and therefore reflects both road extent and speed-limit conditions.

Because consistent measurements of effective walking width were unavailable, road type and hierarchy were used to represent roadside space availability. Open-space paths, arterial roads, secondary arterial roads, local roads, and crossing connections were assigned scores of 5, 4, 3, 2, and 1, respectively. This ordinal classification represents relative space provision potential rather than measured unobstructed walking width.

Path continuity was quantified using continuous-route length. At-grade crossing links (Figure 3) were retained for topological connectivity but treated as interruptions when measuring continuous walking routes, whether signalized or unsignalized. These links were assigned their own short lengths and did not join the adjoining sidewalk routes into one continuous route. Along the same sidewalk, continuity was maintained where no road

crossing was required; the two sides of a T-intersection were therefore assessed separately. Pedestrian overpasses and underpasses preserved continuity across roads.

Where no such interruption occurred, routes through branches followed the continuation of the same road name or road hierarchy, rather than including all connected branches. Loops were measured once around the circuit. The total length of each identified continuous route was assigned to its constituent GIS segments, even when topological nodes divided the route into several shorter segments, including those associated with pedestrian overpasses and underpasses.

Raster-based indicators represented slope, crowding, nighttime light intensity, and vegetation coverage. Baidu heatmap intensity was used as an area-level proxy for pedestrian activity and potential crowding [34], rather than a direct measurement of crowding on individual paths. The 38 hourly heatmap rasters were averaged with equal weights at each raster cell. Similarly, the speed-limit-based indicator represents potential traffic interference rather than observed traffic volume, and nighttime light intensity represents surrounding nighttime brightness rather than path-level illuminance, lighting uniformity, or glare. Vegetation coverage represents the vegetation component of the survey attribute but does not directly measure pedestrian-view greenery. These indicators operationalize the environmental dimensions examined in the CBC experiment while retaining the limitations of city-scale proxy measurements.

2.5.2. Standardization and Integrated Fitness Suitability Assessment

For the fitness suitability assessment, all quantified indicators were assigned to the refined walking network, with each road segment serving as the basic evaluation unit. Indicators derived from the 500 m × 500 m fishnet grid were assigned to the corresponding road segments using spatial joins, while raster-based indicators were represented by the mean raster values along each segment. Topology-based indicators were calculated directly from the refined walking network. After this mapping process, each road segment contained values for all eight fitness suitability indicators, providing a consistent basis for the subsequent assessment.

Because the indicators differed in measurement units and ranges, min–max normalization was used to express their relative positions within the study dataset on a common 0–1 scale. Positive and negative indicators were transformed using Equations (6) and (7), respectively, so that higher standardized values consistently represented more favorable conditions under the adopted assessment assumptions.

$$X'_{ki} = \frac{X_{ki} - X_{i,\min}}{X_{i,\max} - X_{i,\min}} \tag{6}$$

$$X'_{ki} = \frac{X_{i,\max} - X_{ki}}{X_{i,\max} - X_{i,\min}} \tag{7}$$

where X'_{ki} is the normalized value of indicator i for road segment k; X_{ki} is its original value; and $X_{i,\min}$ and $X_{i,\max}$ are the minimum and maximum values of indicator i across all road segments, respectively. After normalization, all indicators had a consistent evaluation direction, with higher values indicating greater fitness suitability.

The mean individual importance scores calculated in Section 2.3.2 were adopted as preference-informed weights for the corresponding GIS indicators. The qualitative CBC levels were not assigned physical thresholds in the GIS data. Instead, the attribute meanings and preference directions informed the spatial interpretation, while their mean importance scores determined the relative contributions to the composite assessment. The FSI was calculated as follows:

$$FSI_k = \sum_{i=1}^{n} w_i X'_{ki} \tag{8}$$

where FSI_k is the fitness suitability index of road segment k, w_i is the mean individual importance weight, X'_{ki} is the standardized indicator value, and $n = 8$. Higher FSI values indicate greater relative suitability according to the selected criteria. The index is a preference-informed planning score, rather than a CBC prediction of route-choice probability or health benefit. Its additive form assumes compensatory contributions among indicators, and the linear scaling provides a transparent approximation rather than evidence of linear preferences over physical environmental measurements. Because CBC importance depends on the attribute levels included in the experiment, transferring these weights to GIS indicator ranges remains an assessment assumption examined through sensitivity analysis.

Sensitivity analysis was conducted for all 19,846 road segments using the retained standardized indicators. The baseline FSI was compared with an equal-weight assessment and 16 weight-perturbation scenarios, in which each weight was separately multiplied by 0.8 or 1.2 and the complete weight vector was renormalized to sum to one. Four additional scenarios separately transformed the standardized nighttime-light or crowding suitability values using square-root and square functions, while holding the other indicators and weights constant. These transformations tested alternative monotonic scoring shapes and were not fitted CBC utility functions. Stability was assessed using Spearman rank correlation and the proportion of baseline top-ranked segments retained among the highest-scoring 20% of segments (3970 segments). This percentage was used only as a common comparison criterion, not as a route-selection threshold.

2.6. HPT Network Generation

2.6.1. Connection Node Extraction

To generate an HPT network that reflects the spatial organization of residents' walking-based fitness activities, key connection nodes were first identified. These nodes represent major locations associated with walking-based fitness activities and spatial transitions. Considering residents' daily activity patterns and the role of everyday destinations in active mobility [35], four types of connection nodes were identified: residential nodes, workplace nodes, public transport nodes, and open-space nodes. Depending on their spatial characteristics, these nodes were extracted from MSSD using two approaches: spatial density analysis and key-node selection (Table 4).

Table 4. Classification and extraction methods of connection nodes.

Node Type	Functional Role	Data Source	Extraction Method
Residential nodes	Major starting locations for residents' walking-based fitness activities	Residential POIs	Density analysis to identify clusters of residential POIs
Workplace nodes	Major activity anchors for residents on working days	Office-related POIs	Density analysis to identify clusters of office-related POIs
Public transport nodes	Major connection points between public transport and walking-based fitness activities	Bus-stop POIs	Density analysis to identify clusters of bus stops
		Metro-station POIs	Selection of metro stations with transfer functions
Open-space nodes	Major destinations for walking-based fitness activities	Open-space POIs	Selection of urban parks, civic squares, and natural scenic areas with ≥500 user reviews

Kernel density analysis was conducted separately for residential, office-related, and bus-stop POIs, using a 500 m search radius and a 50 m output cell size. The resulting

density surfaces were classified into five levels using the Natural Breaks (Jenks) method in GIS. The highest-density areas were extracted, and their geometric centroids were used as connection nodes. For nodes identified through key-node selection, metro stations with transfer functions were selected as public transport nodes. Dianping review data have been shown to provide useful information on park visitation and public use [36]; therefore, urban parks, civic squares, and natural scenic areas with ≥500 user reviews were selected as open-space nodes.

The extracted nodes were automatically located on the nearest walkable network segment. Nearby nodes representing different functions were retained without distance-based merging.

2.6.2. Identification and Integration of High-Continuity Spaces

To enhance the capacity of the generated network to support sustained walking-based fitness activities, existing urban spaces with high continuity potential were identified and incorporated into HPT network generation as complementary spatial resources. Walking-based fitness activities often benefit from continuous movement, maintenance of a relatively stable pace, and fewer interruptions from road crossings [12,23]. Linear spaces with longer continuous paths and fewer interruptions may therefore provide more favorable conditions for sustained walking-based fitness activities [12,23]. A previous study recommended that Chinese adults walk continuously for at least 30 min per day at a cadence of ≥110 steps/min [37]. Using a mean adult step length of approximately 0.70 m reported in another study [38], walking at this cadence for 30 min corresponds to an estimated distance of approximately 2.31 km. The estimated distance of 2.31 km was used as a design reference for this walking scenario, rather than as a screening threshold or a minimum route length required for health benefits.

Meanwhile, improving the overall continuity of the HPT network through the reuse of existing urban spaces is consistent with the broader objective of activating underutilized spatial resources in the context of urban regeneration [39,40]. This study adopts the four-type classification established in the authors' earlier continuity-oriented planning study in Qingdao [19]: railway-related spaces, spaces beneath elevated roads, riverfront and coastal spaces, and spaces along the outer boundaries of large landscape areas. The typology and its continuity rationale are inherited methodological components. In the present framework, these spatial resources are identified from OSM vector data and integrated with routes generated using the eight-indicator FSI and the expanded daily activity node system. Their role is to complement suitability-based route generation with opportunities for longer continuous walking corridors.

The four spatial types were identified as potential planning corridors. Railway-related spaces, spaces beneath elevated roads, and riverfront and coastal spaces primarily support proposed paths following their linear spatial structure, while reusing existing paths where available [39,40]. Routes around large landscape areas primarily follow existing peripheral paths supplemented by proposed connections to form loops. Unresolved barriers and dead ends remain discontinuities. The resulting corridors therefore combine existing paths and proposed development, rather than representing entirely existing continuous trails.

2.6.3. Route Generation

HPT routes were generated by using the identified connection nodes as locations to be linked, the refined walking network as the underlying network, and the identified high-continuity spaces as complementary spatial resources. Through the integration of these elements, an HPT network was generated that considers both residents' daily activity needs

and the environmental suitability for walking-based fitness activities. Figure 4 schematically illustrates the integration of these spatial elements in the HPT network-generation process.

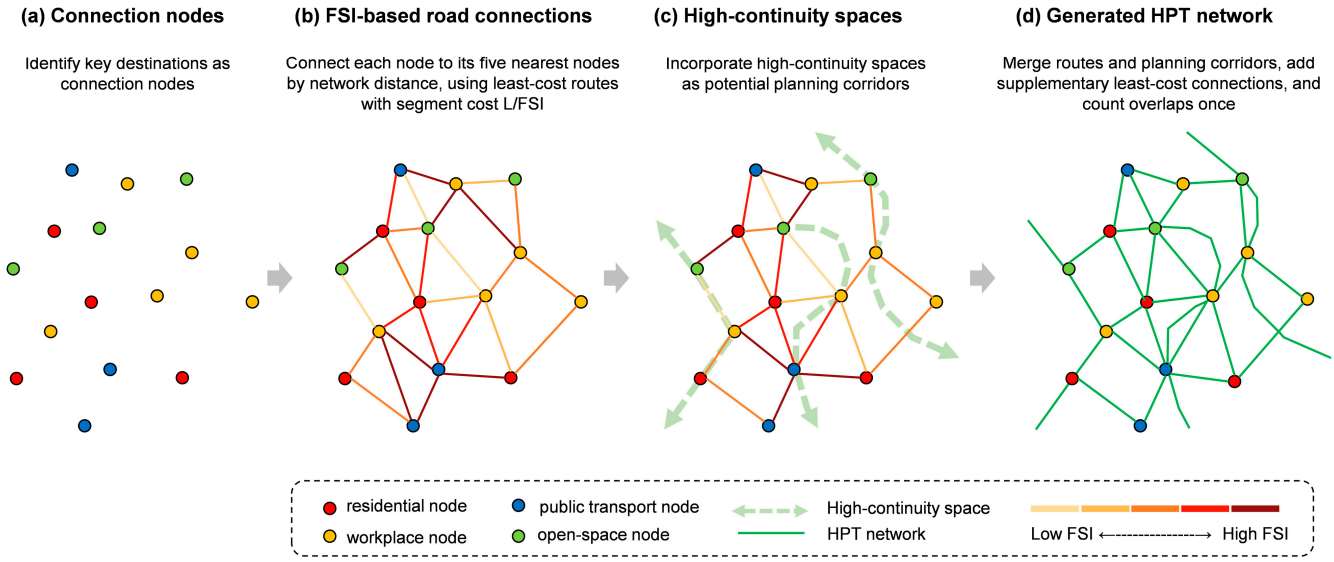


Figure 4. Schematic illustration of HPT network generation.

An impedance-based least-cost routing strategy was applied [13]. Each of the 77 connection nodes was paired with its five nearest other nodes, measured by shortest distance on the refined walking network. Removing self-pairs and reciprocal duplicates yielded 258 undirected node pairs, each routed independently. The cost of a candidate route P was calculated as follows:

$$C(P) = \sum_{e \in P} \frac{L_e}{FSI_e} \quad (9)$$

where L_e is the actual geometric length (m) of segment e and FSI_e is its fitness suitability score. This length differs from the continuous-route length assigned for continuity assessment. All FSI values were positive (0.2456–0.8788), so no zero-value adjustment was required. The route with the lowest total cost was selected for each pair.

Overlapping route sections were merged and counted once. The four types of planning corridors were then incorporated. Supplementary links were generated using closest-facility analysis with the same cost between selected corridor locations and candidate locations on the FSI-based network; 18 connection routes were retained. Overlaps were removed again after integration. Unconnected corridor sections were retained as planning opportunities without assuming verified access.

2.6.4. Scenario Comparison and Sensitivity Analysis

Three generated scenarios were compared: shortest-distance routing, FSI-based routing before corridor integration, and the full planning framework. The first two used the same 77 nodes and 258 pairs; the full scenario additionally incorporated planning corridors and supplementary links. The existing refined walking network was included as a descriptive reference. Generated network length was measured after removing overlaps. FSI and the source-network continuity score were averaged by geometric segment length. Geometric connectivity was summarized by the number of shared-vertex components and the length share of the largest component, using coordinates rounded to 0.001 m.

To examine coverage at comparable network lengths, a supplementary length-constrained integration scenario retained the entire FSI-based network and used the shortest-distance network's unique length as a cap. Eligible units were whole single-part corridors

sharing line geometry with the FSI-based network. They were ordered by net added length relative to that network, with ties resolved by corridor category and source-record order. Each corridor was added only if the merged network remained within the cap; overlaps were counted once. Selection did not use coverage outcomes. This scenario represents partial corridor integration rather than the full planning scenario (Table S3).

Route-generation sensitivity was assessed using two alternative settings: equal weights (1/8 for each indicator) with the original 77 nodes, and raising the open-space review threshold from 500 to 1000 while retaining the original CBC weights and other node-selection criteria. Five-nearest-node pairs were recomputed for the reduced node set. Each result was compared with the baseline FSI routing scenario using unique network length, mean FSI evaluated with the original CBC weights, and length-weighted Jaccard overlap (shared length divided by union length). These tests were confined to the FSI routing stage.

2.7. Euclidean Proximity Coverage Evaluation

Service potential was evaluated using Euclidean proximity thresholds of 360, 576, and 1080 m. These distances correspond to 5, 8, and 15 min at an assumed walking speed of 1.2 m/s [41], but were used as distance references rather than actual walking-time estimates. The 576 m threshold was retained with reference to Qingdao's "8-min fitness circle" initiative [20], without treating proximity coverage as evidence of policy compliance.

For each scenario, buffers around the network were overlaid with residential POIs to count covered locations and their estimated population. Residential coverage percentages used all 2764 included locations as the denominator. In the reverse analysis, buffers around all residential POIs were merged, and the unique network length within them was measured as a proportion of each scenario's total unique length. Overlapping residential buffers did not lead to repeated counting of network sections.

Population at each residential location was estimated by multiplying its household count, obtained from property websites in 2025, by the district-level mean household size from the 2020 Seventh National Population Census: 2.41 persons per household for Shinan and Shibei, 2.55 for Licang, and 2.38 for Laoshan. A residential point inside a buffer contributed its full estimated population and was counted only once per distance threshold. Population coverage percentages used the total estimated population of all included residential locations as the denominator.

Euclidean buffers were used to provide a consistent city-scale screening of spatial proximity across the network scenarios. Although the refined walking network supports routing between selected nodes, usable entrances and residential access connections to the planning corridors have not been comprehensively verified. The evaluation therefore measures proximity to mapped routes rather than actual pedestrian-network accessibility [42,43].

3. Results

3.1. Relative Importance and Indicator Weights

Table 5 reports the mean attribute importance scores and their approximate 95% confidence intervals, verified using the CBC outputs associated with the earlier investigation [18]. Path continuity had the highest mean importance, followed by crowding, vegetation-related landscape conditions, and slope. These preference estimates are used as assessment inputs and are not presented as findings from a new survey.

Individual importance scores were averaged and converted into decimal weights for the corresponding GIS indicators. The confidence intervals describe uncertainty in the mean importance scores arising from between-respondent variation. The spatial assessment and scoring sensitivity results obtained using these inputs are reported in Section 3.2.

Table 5. Mean CBC attribute importance, approximate 95% confidence intervals, and GIS assessment weights.

Indicator	Relative Importance (%)	95% CI (%)	Weight
Facility mix	9.70	9.05–10.35	0.0970
Slope	12.96	12.13–13.79	0.1296
Roadside space availability	10.67	10.20–11.15	0.1067
Path continuity	20.64	19.49–21.80	0.2064
Crowding	14.86	13.79–15.94	0.1486
Traffic flow impact	10.20	9.60–10.80	0.1020
Nighttime light intensity	7.34	6.85–7.82	0.0734
Vegetation coverage	13.62	12.82–14.42	0.1362

Note: Estimates were verified against the archived individual-level CBC outputs ($N = 442$). The 95% confidence interval (CI) for each mean percentage importance estimate was calculated using the normal approximation. Displayed importance scores and weights are rounded; their totals may therefore differ slightly from 100% or 1. GIS calculations used weights rounded to seven decimal places.

3.2. Fitness Suitability

Figure 5 shows the spatial distributions of the eight indicators as min–max normalized values in their original environmental directions. Darker colors indicate higher indicator values, which do not necessarily represent greater fitness suitability. Each panel uses five Natural Breaks (Jenks) classes, with numerical ranges shown in its legend. Facility mix, traffic flow impact, crowding, and nighttime light intensity generally showed higher values in more intensively developed urban areas, with values tending to decrease toward the urban periphery. Facility mix and nighttime light intensity exhibited polycentric concentration patterns across the urban area, whereas higher levels of crowding and traffic flow impact were concentrated in the old urban area and other high-density built-up areas. These patterns suggest that central urban areas generally provide greater facility availability for walking-based fitness activities, while also being associated with greater crowding and traffic-related disturbance.

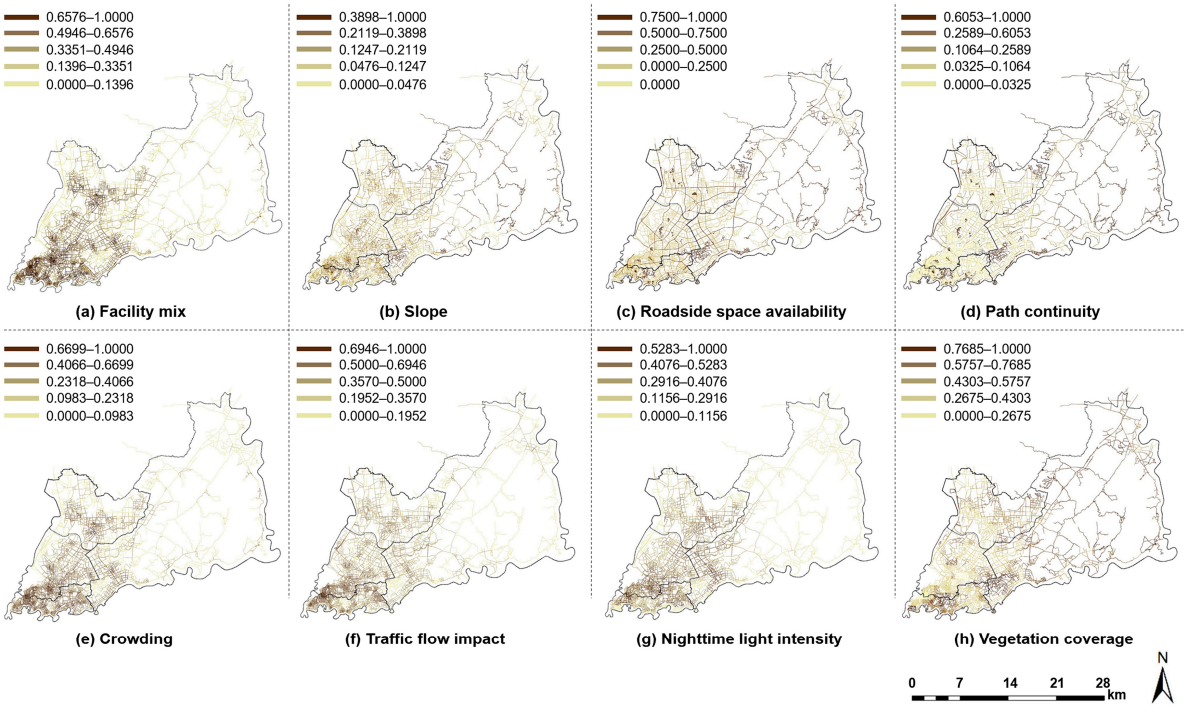


Figure 5. Spatial distributions of the eight fitness suitability indicators.

Slope and vegetation coverage showed spatial patterns more closely associated with natural topography and ecological conditions. Slope was generally lower in the western part of the study area and higher in the east. Vegetation coverage was concentrated in natural areas such as coastal parks, forest parks, and mountainous scenic areas, forming high-value clusters around large ecological patches, whereas the central urban area generally exhibited lower vegetation coverage.

In contrast, roadside space availability and path continuity primarily reflected structural characteristics of the walking environment. Roadside space availability, which was derived from road type and hierarchy, exhibited an overall grid-like spatial pattern. Path continuity was generally lower in the central urban area and higher along the urban periphery, coastal and riverfront areas, and suburban natural areas. Of all segments in the base walking network, 12.26% had assigned continuous-route lengths of at least 2.31 km, the reference described in Section 2.6.2, indicating limited provision of long continuous walking segments in the existing walking environment.

After direction alignment, the mean standardized scores further characterized the relative suitability of the assessed environmental conditions. Slope and crowding had relatively high mean standardized scores (0.8952 and 0.7720, respectively), indicating comparatively favorable conditions for walking-based fitness activities with respect to these two indicators. In contrast, path continuity had the lowest mean standardized score (0.1332). Together with its highest relative importance (20.64%), this result highlights a marked imbalance between the existing provision of continuous walking space and the relative importance assigned to path continuity in respondents' choices, suggesting that path continuity warrants particular attention in subsequent HPT network generation.

Overall, the indicators exhibited substantial differences in both spatial distribution and mean standardized scores, reflecting different dimensions of fitness suitability. The weighted indicators were subsequently integrated to derive the overall FSI. For visualization, FSI values were classified into five classes using the Natural Breaks (Jenks) method. The resulting spatial pattern of fitness suitability is shown in Figure 6. Areas with relatively high FSI values were primarily distributed along coastal open spaces, around large parks, and along some major urban roads, forming several linear spaces with relatively high fitness suitability. Road segments with moderate FSI values were widely distributed across peripheral built-up areas and the major road network, forming transitional spaces between areas with relatively high fitness suitability. Low-FSI road segments were mainly concentrated in high-density built-up areas characterized by greater traffic disturbance and lower path continuity.

The segment-level assessment showed relatively stable rankings across the tested weighting and scoring scenarios. The equal-weight assessment produced a Spearman correlation of 0.9654 with the baseline FSI and retained 92.44% of the baseline top-ranked 20% of segments. Across the 16 weight-perturbation scenarios, correlations ranged from 0.9970 to 0.9999 and top-segment retention ranged from 96.93% to 99.22%. The four nonlinear nighttime-light and crowding scoring scenarios yielded correlations of 0.9889–0.9936 and retention of 95.26–97.41%. These results concern segment rankings; route-generation sensitivity is reported in Section 3.5.

3.3. Connection Nodes

A total of 77 connection nodes were identified: 16 residential nodes, 14 workplace nodes, 18 public transport nodes comprising five bus-stop-cluster nodes and 13 metro transfer stations, and 29 open-space nodes (Figure 7). Overall, all four types showed spatially concentrated distribution patterns, although the locations of these concentrations differed. Residential and workplace nodes were primarily concentrated in Shibei and Licang districts and showed broadly similar spatial distributions, indicating broadly overlapping

spatial concentrations in these areas. Public transport nodes were mainly identified in areas with high concentrations of bus stops and around major metro transfer stations and were generally located near residential and workplace nodes. Their spatial proximity to residential and workplace nodes suggests potential for integrating public transport access with the HPT network, particularly in relation to first- and last-mile walking. In contrast, open-space nodes were mainly distributed along the southern coastal area and in natural areas such as Laoshan in the eastern part of the study area, forming relatively independent spatial concentrations with limited overlap with the main concentrations of residential and workplace nodes.

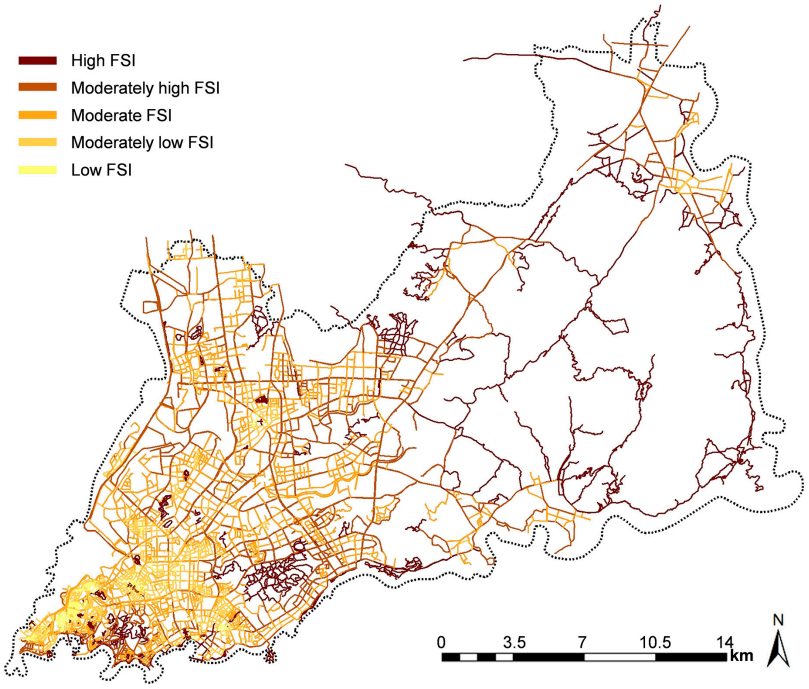


Figure 6. Spatial distribution of the FSI.

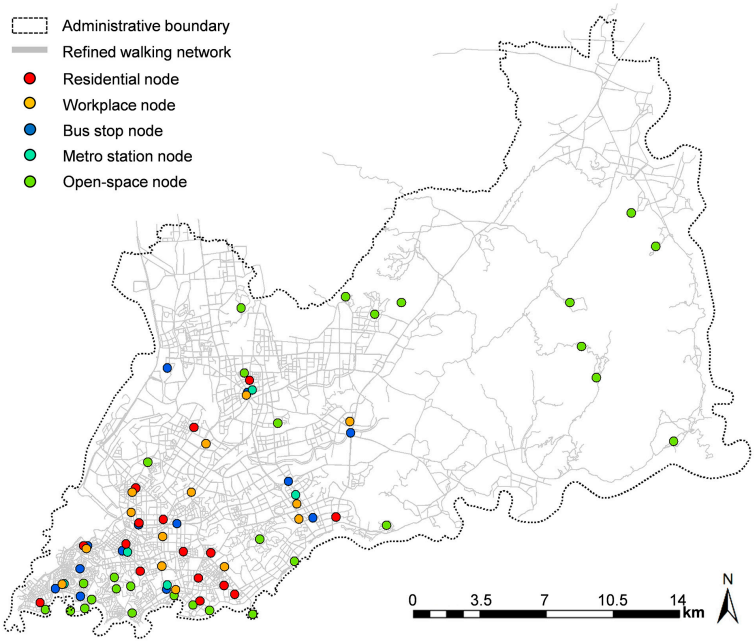


Figure 7. Spatial distribution of connection nodes.

3.4. High-Continuity Spaces

Four types of existing urban spaces with high continuity potential were identified and integrated: railway-related spaces, spaces beneath elevated roads, riverfront and coastal spaces, and spaces along the outer boundaries of large landscape areas.

The spatial distribution of the integrated high-continuity spaces is shown in Figure 8. A total of 3 railway-related segments, 10 segments beneath elevated roads, 34 riverfront and coastal segments, and 23 segments along the outer boundaries of large landscape areas were identified. All four types offered potential continuous corridors that could be incorporated into the HPT network. Riverfront and coastal spaces and spaces along the outer boundaries of large landscape areas generally formed longer continuous walking corridors, whereas railway-related spaces and spaces beneath elevated roads primarily provided local connections within built-up areas, linking otherwise discontinuous walking spaces.

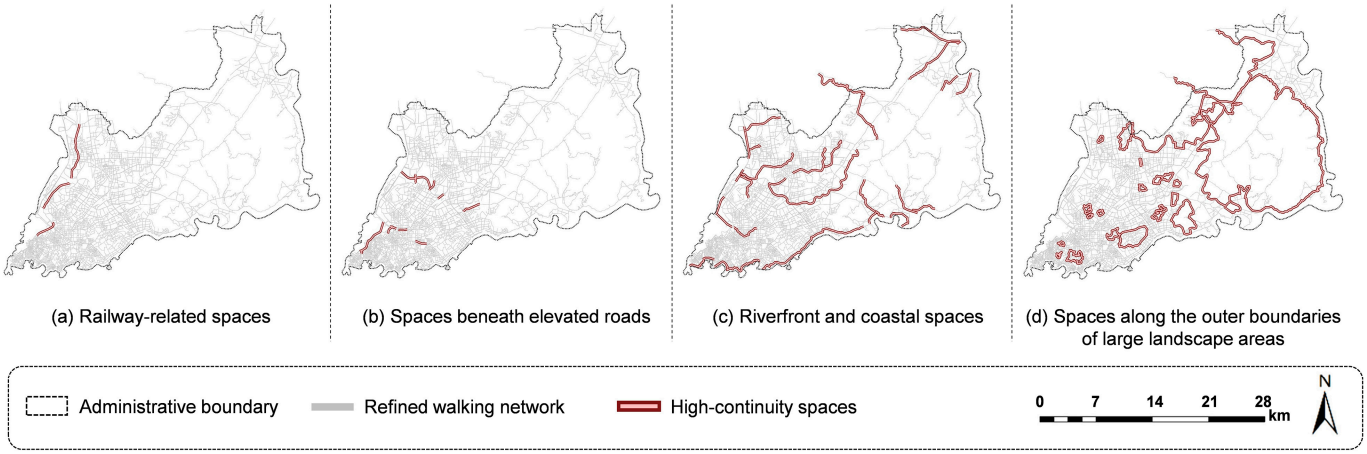


Figure 8. Spatial distribution of potential high-continuity planning corridors.

The maximum geometric route lengths in the four categories were 7.13, 5.89, 16.12, and 78.90 km, respectively. The 78.90 km route is a proposed circuit around the Laoshan Scenic Area, combining existing paths and proposed connecting sections. Of the 70 identified planning routes, 50 (71.43%) had geometric lengths of at least 2.31 km. These lengths describe the planning scenario rather than verified current continuous walkability.

3.5. HPT Network

The FSI-based routing stage generated a 374.26 km network linking the 77 connection nodes. Integrating the four types of planning corridors and 18 supplementary connection routes produced a full planning scenario of 777.09 km, after counting overlapping sections once (Figure 9). The planning corridors include existing paths and proposed paths or connections. These corridors provide a spatial basis for planning longer continuous walking routes within the proposed HPT network.

Table 6 compares the existing-network reference and the three generated scenarios. The FSI-based network had a higher length-weighted mean FSI (0.5845 vs. 0.5687) and mean source continuity score (0.3837 vs. 0.3375) than the shortest-distance network, with 5.44% less unique network length. However, the total distance across the 258 individual routes was 0.93% greater, reflecting greater reuse of shared sections after merging.

The two routing scenarios each formed one shared-vertex component. The full scenario comprised 17 geometric components, with 91.20% of its length in the largest component; it should therefore be interpreted as a main network with additional planning corridors rather than a fully connected existing trail network.

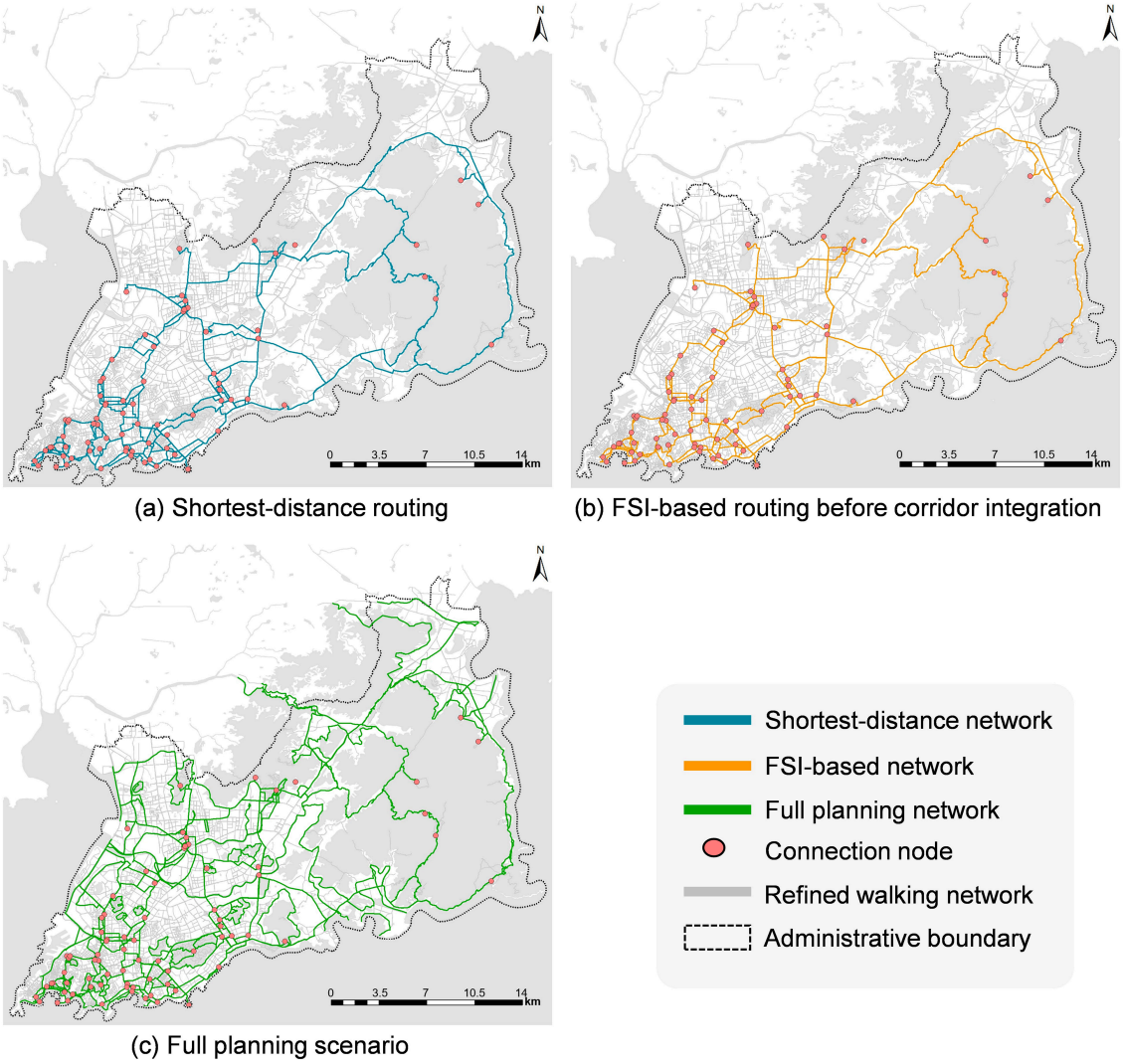


Figure 9. Spatial distribution of the three HPT network scenarios.

Table 6. Comparison of the existing walking network and the three generated scenarios.

Scenario	Network Length (km)	Mean FSI	Mean Source Continuity Score	Geometric Components	Largest Component Length Share (%)
Existing-network reference	3372.11	0.5213	0.2131	16	99.60
Shortest-distance routing	395.79	0.5687	0.3375	1	100.00
FSI-based routing	374.26	0.5845	0.3837	1	100.00
Full planning scenario	777.09	—	—	17	91.20

Note: Mean FSI and mean source continuity score are weighted by geometric segment length. Source continuity characterizes the original continuous walking spaces and does not measure uninterrupted walking within the selected network. Components describe shared-vertex geometry, not verified pedestrian access. Source scores are available for only 69.71% of the full scenario, so its whole-network means are not reported. The existing network is a descriptive reference; these comparisons do not control total network length. A supplementary length-constrained coverage comparison is reported in Section 3.6 and Table S3.

The two sensitivity tests produced network lengths within 2.16% of the baseline and mean FSI values of 0.5820–0.5840 (Table 7). Length-weighted Jaccard overlap was 86.29%

for equal weights and 78.84% for the raised open-space threshold. Thus, overall extent and mean FSI changed little in these tests, but specific routes were more sensitive to the node-selection criterion.

Table 7. Sensitivity of the FSI-based routing stage to indicator weights and the open-space selection threshold.

Metric	Baseline	Equal Weights	Open Spaces with ≥1000 Reviews
Connection nodes	77	77	67
Node pairs	258	258	224
Unique network length (km)	374.26	378.72	366.18
Length change from baseline (%)	0.00	+1.19	−2.16
Mean original-CBC FSI	0.5845	0.5820	0.5840
Length-weighted Jaccard overlap (%)	100.00	86.29	78.84

Note: All mean FSI values use the original CBC weights and are length-weighted. Jaccard overlap is the shared network length divided by the union length of the alternative and baseline networks. Corridor integration and supplementary connections were not rerun in these sensitivity tests.

3.6. Euclidean Proximity Coverage

Table 8 reports Euclidean proximity coverage for the full planning scenario. At 360, 576, and 1080 m, the network covered 82.34%, 94.25%, and 99.13% of the included residential locations, corresponding to 75.92%, 89.24%, and 98.11% of their total estimated population, respectively. At 1080 m, 24 residential locations with an estimated population of 58,670 remained outside the proximity range.

Table 8. Euclidean proximity coverage of the full planning scenario.

Euclidean Proximity Threshold (m)	Network Within Residential Proximity Buffers		Residential Locations Within Network Proximity Buffers		Estimated Population Within Network Proximity Buffers	
	Length (km)	Proportion (%)	Number	Proportion (%)	Population	Proportion (%)
360	373.80	48.10	2276	82.34	2,351,998	75.92
576	441.51	56.82	2605	94.25	2,764,851	89.24
1080	524.57	67.50	2740	99.13	3,039,520	98.11

Note: Residential and population coverage use 2764 locations and 3,098,190 estimated residents as denominators. Network-length shares use the full scenario's unique length of 777.09 km. Residential buffers were merged before measuring network length; each network section was counted once per threshold. Lengths and percentages are rounded independently.

Conversely, 373.80, 441.51, and 524.57 km of the full planning network lay within the merged 360, 576, and 1080 m residential buffers, accounting for 48.10%, 56.82%, and 67.50% of its total length, respectively. The remaining 252.53 km (32.50%) lay outside the 1080 m residential buffers.

Scenario comparisons are reported in Table S3. At 576 m, shortest-distance routing and FSI-based routing covered 78.40% and 77.64% of residential locations and 68.63% and 68.39% of estimated population, respectively. The length-constrained scenario incorporated seven whole corridors, adding 20.65 km of unique length to the FSI-based network. Its total length was 394.91 km, 0.22% below the shortest-distance network, with residential and population coverage of 78.36% and 68.89%. Coverage was therefore similar at comparable lengths; the full scenario's higher coverage was accompanied by substantially greater network extent. The existing-network reference covered all included residential locations within 360 m Euclidean proximity, although its much greater extent (3372.11 km) limits direct comparison with the generated scenarios.

4. Discussion

4.1. Integrating Fitness Suitability and Spatial Continuity in HPT Network Planning

The spatial assessment identified limited provision of long continuous walking segments in the existing walking environment. Together with the high importance assigned to continuity in the previous CBC study [18], this finding highlights the need to consider continuity in both segment assessment and network organization. As an FSI indicator, continuity contributes to the evaluation of individual road segments alongside other environmental attributes. However, a high overall suitability score does not by itself establish that a segment forms part of a longer continuous walking route. Integrating high-continuity spatial resources therefore complements suitability-based route selection by addressing how selected routes can be organized into longer walking corridors.

Compared with the earlier continuity-oriented planning study [19], the present framework broadens the environmental basis for route selection. The earlier study used continuity grades to determine routing impedance, while slope and vegetation were primarily evaluated after route selection. Here, eight preference-weighted environmental indicators inform the spatial assessment used for routing. The four high-continuity space types are retained from the earlier study and incorporated into this broader assessment and network-generation process. The extension therefore concerns how established preference evidence and continuity-oriented spatial strategies are combined, rather than the identification of new spatial types or the introduction of least-cost routing itself.

The expanded node system further links this environmental assessment with everyday activity locations. Residential, workplace, public transport, and open-space nodes represent potential origins, destinations, and transfer locations, extending the earlier emphasis on metro stations and continuity-related spatial anchors [19]. Their inclusion provides a basis for organizing connections between daily activity spaces and longer walking corridors. Together, the multi-indicator assessment, expanded node system, and continuity-oriented spatial resources constitute an integrated planning process for generating HPT networks within the existing urban fabric.

4.2. Planning Implications of the Generated HPT Network

The full planning scenario covered 94.25% of the included residential locations and 89.24% of their estimated population at 576 m Euclidean proximity, suggesting broad spatial provision near the included residential locations. However, coverage was similar between the length-constrained integration and shortest-distance scenarios, so the full scenario's higher coverage should be interpreted alongside its larger extent. The 252.53 km outside the 1080 m residential buffers may support recreational walking and connections between urban and landscape spaces, extending the network's planning role beyond local residential provision. These functions remain planning opportunities rather than demonstrated patterns of use or health benefits.

While trail and greenway planning has often emphasized the connection of landscape resources and spatial connectivity [13], recent studies have increasingly highlighted the importance of individual mobility and everyday activity destinations in planning active-travel corridors [35]. HPT planning further emphasizes the relationship between residents' daily walking-related fitness needs and the spatial provision of health-promoting environments. Organizing the network around functional spaces associated with residents' daily activities allows HPTs to be located closer to residential areas, workplaces, and public transport nodes, while also providing connections to open spaces and other walking environments. Such spatial organization may reduce the additional time and travel required to access opportunities for walking-based fitness and facilitate the integration of fitness-oriented walking into everyday travel. From this perspective, the planning value of an HPT network lies not

only in improving the spatial conditions for walking-based fitness but also in enhancing access to health-promoting environments [5,42]. This may broaden the role of HPTs from individual walking facilities toward a component of public infrastructure that supports everyday PA and the spatial provision of health-promoting resources [2,5].

4.3. Planning and Implementation Strategies for HPTs

The generated HPT network combined FSI-based routes on the refined walking network with potential high-continuity planning corridors and supplementary connections. The FSI-based routes formed the primary connecting system, while the planning corridors were intended to strengthen network-level spatial continuity. Among these high-continuity spaces, railway-related spaces and spaces beneath elevated roads primarily provided local linear connections within built-up areas, whereas riverfront and coastal spaces and spaces along the outer boundaries of large landscape areas offered potential for longer continuous walking corridors. These differences suggest that HPT planning should move beyond a uniform approach toward function-oriented and differentiated implementation, with interventions tailored to the roles that different types of spaces play in network connection and continuity.

For FSI-based routes, priority should be given to improving walking conditions and connections with relevant nodes in coordination with the existing active-mobility system [35], supporting their role as the basic connecting framework of the HPT network. For infrastructure-related spaces, such as railway-related spaces and spaces beneath elevated roads, interventions should focus on the adaptive reuse of existing spaces [39,40], the connection of discontinuous segments, and the integration of multiple functions to strengthen their role in network connectivity. For open spaces such as riverfront and coastal spaces and spaces along the outer boundaries of large landscape areas, priority should be given to maintaining their continuous spatial edges and making use of their inherent continuity, while strengthening connections with surrounding spaces and urban roads to support overall network continuity and service potential. Differentiated strategies for these spatial types could make better use of their respective spatial characteristics and existing spatial resources, thereby potentially improving the adaptability and feasibility of HPT network implementation.

The structure of the generated network also suggests a phased implementation strategy in which the main network framework is established first and progressively extended into a finer-grained network. High-continuity spaces can serve as major continuous corridors, while urban roads provide broader network extension and service coverage. Accordingly, priority could be given to feasible sections serving densely populated communities with unmet local walking needs, followed by peripheral recreational corridors and connections between urban and landscape spaces. This approach could support a progressively developed network extending from major continuous corridors to surrounding urban spaces, while reducing the difficulty of simultaneous network-wide implementation and allowing subsequent sections to be adjusted according to actual use and local conditions.

Finally, the proposed HPT network combines existing roads and paths with proposed development within available urban spatial corridors. This finding highlights the potential value of spatial sharing and the coordinated use of limited urban space in HPT implementation. In existing built-up areas, HPTs could be coordinated with active-mobility systems, public transport, and public open spaces [35,44]. Depending on local spatial and usage conditions, HPT implementation could consider either separated or shared arrangements to accommodate walking-based fitness alongside cycling and other active-mobility activities. Implementation based on the integration and shared use of existing spatial resources may

therefore provide an adaptable pathway for the continued development of HPT networks in existing urban areas [39,40].

4.4. Limitations and Future Research

Despite its contribution to the quantitative and systematic planning of HPTs, this study has several limitations. First, the analysis was conducted in the eastern urban area of Qingdao, which is characterized by a combination of coastal and mountainous environments and densely built-up areas. Given that cities may differ in urban form, natural conditions, and walking behavior, the applicability of the proposed indicator system and the transferability of the identified types of high-continuity spaces need to be further examined in other urban contexts [45].

Second, the city-scale proxies do not directly measure effective walking width, traffic volume, path-level lighting, on-path crowding, or pedestrian-view greenery. Pavement material and maintenance conditions were also not assessed. The FSI should therefore be interpreted as a screening assessment of selected environmental dimensions, rather than a comprehensive audit of route usability.

Differences in dataset dates and resolutions, together with the two-day heatmap sampling, limit temporal and spatial representativeness [46]. Population coverage relies on point-based estimates. Euclidean buffers do not account for detours, barriers, crossing delays, or entrance restrictions and therefore do not establish actual walking accessibility. Coverage involving proposed corridors represents planning potential rather than verified current access. The planning corridors also include proposed paths whose key gaps, entrances, and access restrictions have not been comprehensively verified. The sensitivity tests cover only two alternative settings at the FSI route-generation stage and do not establish robustness of the entire planning framework. The length-constrained comparison evaluates coverage under one partial-integration rule and does not establish comparable-length performance of the complete framework across all dimensions.

In addition, this study primarily evaluated the spatially generated HPT network and its potential service coverage, without validating network performance through actual use after implementation. The CBC experiment reflects respondents' stated preferences for attributes of the walking environment, but whether the generated network would increase actual use frequency, walking duration, or levels of PA requires further validation using longitudinal behavioral data [47]. Future research could conduct cross-case validation in different cities, integrate mobility trajectories, field surveys, and dynamic environmental data to refine indicator measurement [48], and evaluate the effects of the generated network on actual walking behavior and health outcomes through pilot implementation, post-implementation evaluation, and before-and-after comparisons [2,47]. Land ownership, construction costs, and engineering feasibility could also be incorporated as additional constraints to facilitate the translation of planning results into feasible implementation strategies.

5. Conclusions

The primary goal of HPT planning is not merely to identify individual routes suitable for walking, but to develop an interconnected trail network that provides suitable and continuous spatial support for residents' walking-based fitness activities. To address the limited integration of route-level environmental assessment, network generation, and service potential evaluation in current HPT planning, this study developed a data-driven planning framework for generating HPT networks using multi-source spatial data. The framework used fitness participants' environmental preferences to determine indicator weights, assessed the fitness suitability of the existing walking network, incorporated connection nodes to organize connections among functional spaces associated with residents'

daily walking activities, and integrated existing urban spaces with high continuity potential into network generation. The service potential of the generated network was subsequently evaluated through Euclidean proximity coverage of residential locations and estimated population, together with network length within residential proximity buffers. In this way, the proposed framework extends HPT planning from the identification of suitable routes toward an integrated process encompassing fitness suitability assessment, network generation, and service potential evaluation.

The FSI-based routing stage generated a 374.26 km network with higher length-weighted fitness suitability and mean source continuity than the shortest-distance alternative. Integrating planning corridors and supplementary connections produced a 777.09 km planning scenario, with 91.20% of its length in the largest geometric component. At 576 m Euclidean proximity, it covered 94.25% of included residential locations and 89.24% of their estimated population; at 1080 m, these proportions were 99.13% and 98.11%. The length-constrained integration and shortest-distance scenarios showed similar coverage, indicating that the full scenario's greater coverage should be interpreted alongside its larger network extent.

Overall, the findings suggest that HPT planning should move beyond the suitability-based selection of individual routes toward an integrated, network-based planning process that incorporates spatial continuity and network organization and evaluates the service potential of the resulting network. By incorporating connection nodes and existing urban spatial resources into this process, the proposed data-driven planning framework links route-level environmental assessment with network generation and subsequent service potential evaluation. This framework provides a systematic analytical pathway for generating HPT networks that respond to the spatial requirements of walking-based fitness activities. It contributes to sustainable urban planning by informing the coordinated use of existing urban spatial resources for everyday PA, with explicit assessment of potential residential service provision.

Supplementary Materials: The following supporting information can be downloaded at https://www.mdpi.com/article/10.3390/su182111281/s1. Table S1: Characteristics of respondents included in the choice-based conjoint (CBC) analysis ($N = 442$); Table S2: An example CBC choice task from the questionnaire template; Table S3: Euclidean proximity coverage of the existing-network reference and planning scenarios.

Author Contributions: Conceptualization, Y.Z.; methodology, Y.Z.; software, Y.Z., L.W. (Linzhen Wei), H.Y. and C.S.; validation, Y.Z., L.W. (Linzhen Wei), H.Y. and C.S.; formal analysis, Y.Z., L.S. and L.W. (Lukai Wang); investigation, Y.Z.; resources, Y.Z. and D.L.; data curation, Y.Z., L.W. (Linzhen Wei), H.Y., C.S. and L.S.; writing—original draft preparation, Y.Z.; writing—review and editing, Y.Z., D.L. and L.W. (Linzhen Wei); visualization, Y.Z., L.W. (Linzhen Wei) and H.Y.; project administration, Y.Z. and D.L.; funding acquisition, Y.Z. All authors have read and agreed to the published version of the manuscript.

Funding: This research was funded by the Shandong Provincial Natural Science Foundation, grant number ZR2024QE422.

Institutional Review Board Statement: Ethical review and approval were waived for this study by Institution Committee as per Measures for Ethical Review of Life Science and Medical Research Involving Human Beings.

Informed Consent Statement: Informed consent for participation was obtained from all subjects involved in the study.

Data Availability Statement: The data supporting the findings of this study are available from the corresponding author upon reasonable request.

Acknowledgments: The authors would like to thank all participants who took part in the original CBC survey for their time and cooperation. The authors thank Xingtian Wang of The University of Kitakyushu for the academic guidance he provided on this study during the collaborative research project between Agencysoft Co., Ltd., and The University of Kitakyushu. During the preparation of this manuscript, the authors used ChatGPT (GPT-6.1 Sol, OpenAI, San Francisco, CA, USA) for language refinement. The authors have reviewed and edited the output and take full responsibility for the content of this publication.

Conflicts of Interest: During the collaborative research project between Agencysoft Co., Ltd., and The University of Kitakyushu, Xingtian Wang of The University of Kitakyushu provided academic guidance on this study. The authors declare no conflicts of interest.

Abbreviations

The following abbreviations are used in this manuscript:

HPT	Health-Promoting Trail
MSSD	Multi-Source Spatial Data
PA	Physical Activity
SDGs	Sustainable Development Goals
GIS	Geographic Information System
POI	Point of Interest
CBC	Choice-Based Conjoint
FSI	Fitness Suitability Index
OSM	OpenStreetMap
DEM	Digital Elevation Model
NDVI	Normalized Difference Vegetation Index
HB	Hierarchical Bayes
CI	Confidence Interval

References

1. World Health Organization. *WHO Guidelines on Physical Activity and Sedentary Behaviour*; World Health Organization: Geneva, Switzerland, 2020.
2. Zhang, Y.; Koene, M.; Reijneveld, S.A.; Tuinstra, J.; Broekhuis, M.; van der Spek, S.; Wagenaar, C. The impact of interventions in the built environment on physical activity levels: A systematic umbrella review. *Int. J. Behav. Nutr. Phys. Act.* **2022**, *19*, 156. [CrossRef]
3. Paluch, A.E.; Bajpai, S.; Bassett, D.R.; Carnethon, M.R.; Ekelund, U.; Evenson, K.R.; Galuska, D.A.; Jefferis, B.J.; Kraus, W.E.; Lee, I.-M.; et al. Daily steps and all-cause mortality: A meta-analysis of 15 international cohorts. *Lancet Public Health* **2022**, *7*, e219–e228. [CrossRef] [PubMed]
4. Ding, D.; Nguyen, B.; Nau, T.; Luo, M.; del Pozo Cruz, B.; Dempsey, P.C.; Munn, Z.; Jefferis, B.J.; Sherrington, C.; Calleja, E.A.; et al. Daily steps and health outcomes in adults: A systematic review and dose-response meta-analysis. *Lancet Public Health* **2025**, *10*, e668–e681. [CrossRef]
5. Jacob, V.; Reynolds, J.A.; Chattopadhyay, S.K.; Hopkins, D.P.; Brown, D.R.; Devlin, H.M.; Barrett, A.; Berrigan, D.; Crespo, C.J.; Heath, G.W.; et al. Parks, trails, and greenways for physical activity: A Community Guide systematic economic review. *Am. J. Prev. Med.* **2024**, *66*, 1089–1099. [CrossRef]
6. United Nations. *Transforming Our World: The 2030 Agenda for Sustainable Development*; United Nations: New York, NY, USA, 2015; Available online: https://sdgs.un.org/2030agenda (accessed on 26 October 2026).
7. Prince, S.A.; Lancione, S.; Lang, J.J.; Amankwah, N.; de Groh, M.; Jaramillo Garcia, A.; Merucci, K.; Geneau, R. Examining the state, quality and strength of the evidence in the research on built environments and physical activity among adults: An overview of reviews from high income countries. *Health Place* **2022**, *77*, 102874. [CrossRef]
8. Fonseca, F.; Ribeiro, P.J.G.; Conticelli, E.; Jabbari, M.; Papageorgiou, G.; Tondelli, S.; Ramos, R.A.R. Built environment attributes and their influence on walkability. *Int. J. Sustain. Transp.* **2022**, *16*, 660–679. [CrossRef]
9. Basu, N.; Haque, M.M.; King, M.; Kamruzzaman, M.; Oviedo-Trespalacios, O. A systematic review of the factors associated with pedestrian route choice. *Transp. Rev.* **2022**, *42*, 672–694. [CrossRef]
10. Basu, N.; Oviedo-Trespalacios, O.; King, M.; Kamruzzaman, M.; Haque, M.M. What do pedestrians consider when choosing a route? The role of safety, security, and attractiveness perceptions and the built environment during day and night walking. *Cities* **2023**, *143*, 104551. [CrossRef]

11. Nag, D.; Goswami, A.K. How to develop the walking environment for its 'consumers'? A conjoint answer derived from people's perception of link and network. *Sustain. Cities Soc.* **2024**, *100*, 105031. [CrossRef]
12. Gbadamosi, A.R.; Griffiths, B.N.; Clarke-Cornwell, A.M.; Granat, M.H. Defining continuous walking events in free-living environments: Mind the gap. *Sensors* **2022**, *22*, 1720. [CrossRef]
13. Teng, M.; Wu, C.; Zhou, Z.; Lord, E.; Zheng, Z. Multipurpose greenway planning for changing cities: A framework integrating priorities and a least-cost path model. *Landsc. Urban Plan.* **2011**, *103*, 1–14. [CrossRef]
14. Tomczyk, A.M.; Ewertowski, M. Planning of recreational trails in protected areas: Application of regression tree analysis and geographic information systems. *Appl. Geogr.* **2013**, *40*, 129–139. [CrossRef]
15. Yu, C.; Wang, X.; Zheng, Z.; Lau, S.S.Y. How do urban environments impact walkability? An analysis using multi-source data of Beijing. *Land* **2024**, *13*, 2101. [CrossRef]
16. Xu, B.; Shi, Q.; Zhang, Y. Evaluation of the health promotion capabilities of greenway trails: A case study in Hangzhou, China. *Land* **2022**, *11*, 547. [CrossRef]
17. Zhao, Y.; Liu, D. Identification of urban outdoor walking fitness behavior characteristics and environmental demands based on social network data: A case study of seven districts in Qingdao. *Contemp. Archit.* **2021**, *9*, 120–124. (In Chinese)
18. Zhao, Y.; Liu, D. Research on street environment preferred and mechanism of influence based on a choice-based conjoint analysis of outdoor walking fitness. *Archit. J.* **2022**, *S1*, 158–163. (In Chinese)
19. Zhao, Y.; Liu, D.; Yue, N.; Cheng, Z. Mining of urban fitness space and trail development design based on principles of walking continuity: A case study of the central area of Qingdao. *Chin. Landsc. Archit.* **2022**, *38*, 72–77. (In Chinese) [CrossRef]
20. Qingdao Municipal People's Government. *Qingdao Municipal Fitness Implementation Plan (2021–2025)*; Qingdao Municipal People's Government: Qingdao, China, 2021. Available online: https://www.qingdao.gov.cn/zwgk/xxgk/bgt/gkml/gwfg/202112/t20211210_3982633.shtml (accessed on 26 October 2026). (In Chinese)
21. Qingdao Municipal Bureau of Statistics; Qingdao Survey Office of the National Bureau of Statistics. *Qingdao Statistical Yearbook 2021*; China Statistics Press: Beijing, China, 2021. (In Chinese)
22. Qingdao Municipal Bureau of Statistics. *Communiqué of the Seventh National Population Census of Qingdao*; Qingdao Municipal Bureau of Statistics: Qingdao, China, 2021. Available online: https://www.qingdao.gov.cn/zwgk/xxgk/tjj/gkml/tjjd/202106/P020210608330211942028.pdf (accessed on 26 October 2026). (In Chinese)
23. Tudor-Locke, C.; Han, H.; Aguiar, E.J.; Barreira, T.V.; Schuna, J.M., Jr.; Kang, M.; Rowe, D.A. How fast is fast enough? Walking cadence (steps/min) as a practical estimate of intensity in adults: A narrative review. *Br. J. Sports Med.* **2018**, *52*, 776–788. [CrossRef]
24. Van Cauwenberg, J.; De Bourdeaudhuij, I.; Clarys, P.; Nasar, J.; Salmon, J.; Goubert, L.; Deforche, B. Street characteristics preferred for transportation walking among older adults: A choice-based conjoint analysis with manipulated photographs. *Int. J. Behav. Nutr. Phys. Act.* **2016**, *13*, 6. [CrossRef]
25. Paudel, C.; Timperio, A.; Loh, V.; Deforche, B.; Salmon, J.; Veitch, J. Understanding the relative importance of micro-level design characteristics of walking paths in parks to promote walking among older adults. *Urban For. Urban Green.* **2023**, *89*, 128129. [CrossRef]
26. Gidley, A.D.; Lankford, D.E. Cost of transport at preferred walking speeds are minimized while walking on moderately steep incline surfaces. *Hum. Mov. Sci.* **2021**, *79*, 102849. [CrossRef]
27. Sun, S.; Sun, C.; Duives, D.C.; Hoogendoorn, S.P. Neural network model for predicting variation in walking dynamics of pedestrians in social groups. *Transportation* **2023**, *50*, 837–868. [CrossRef]
28. Handy, S.L.; Boarnet, M.G.; Ewing, R.; Killingsworth, R.E. How the built environment affects physical activity: Views from urban planning. *Am. J. Prev. Med.* **2002**, *23*, 64–73. [CrossRef] [PubMed]
29. Louviere, J.J.; Flynn, T.N.; Carson, R.T. Discrete choice experiments are not conjoint analysis. *J. Choice Model.* **2010**, *3*, 57–72. [CrossRef]
30. Tribby, C.P.; Miller, H.J.; Brown, B.B.; Werner, C.M.; Smith, K.R. Analyzing walking route choice through built environments using random forests and discrete choice techniques. *Environ. Plan. B Urban Anal. City Sci.* **2017**, *44*, 1145–1167. [CrossRef]
31. Zhang, H.; Zhang, Y. Pedestrian network analysis using a network consisting of formal pedestrian facilities: Sidewalks and crosswalks. *Transp. Res. Rec.* **2019**, *2673*, 294–307. [CrossRef]
32. Verma, R.; Ukkusuri, S.V. A link criticality approach for pedestrian network design to promote walking. *npj Urban Sustain.* **2023**, *3*, 48. [CrossRef]
33. Chen, L.; Zhang, Z.; Long, Y. Association between leisure-time physical activity and the built environment in China: Empirical evidence from an accelerometer and GPS-based fitness app. *PLoS ONE* **2021**, *16*, e0260570. [CrossRef]
34. Bao, W.; Gong, A.; Zhang, T.; Zhao, Y.; Li, B.; Chen, S. Mapping population distribution with high spatiotemporal resolution in Beijing using Baidu heat map data. *Remote Sens.* **2023**, *15*, 458. [CrossRef]
35. Vatanparast, E.; Shataee Joibari, S.; Salmanmahiny, A.; Hansen, R. Urban greenway planning: Identifying optimal locations for active travel corridors through individual mobility assessment. *Urban For. Urban Green.* **2024**, *101*, 128464. [CrossRef]

36. Huai, S.; Liu, S.; Zheng, T.; Van de Voorde, T. Are social media data and survey data consistent in measuring park visitation, park satisfaction, and their influencing factors? A case study in Shanghai. *Urban For. Urban Green*. **2023**, *81*, 127869. [CrossRef]
37. Wang, H.; Jiang, C.M.; Liu, X.; He, Z.T.; Xu, L.L.; Li, J.J. Walking energy expenditure and recommendation in Chinese adults. *China Sport Sci*. **2013**, *33*, 89–93. (In Chinese) [CrossRef]
38. Zheng, P.; Ducharme, S.W.; Moore, C.C.; Tudor-Locke, C.; Aguiar, E.J. Classification of moderate-intensity overground walking speed in 21- to 85-year-old adults. *J. Sports Sci*. **2022**, *40*, 1732–1740. [CrossRef]
39. García-Mayor, C.; Martí, P.; Castaño, M.; Bernabeu-Bautista, Á. The unexploited potential of converting rail tracks to greenways: The Spanish Vías Verdes. *Sustainability* **2020**, *12*, 881. [CrossRef]
40. Mohamed Anuar, M.I.N.; Abdullah, S.A. Reappropriation of elevated highway residual space through green infrastructure planning. *Plan. Malays*. **2020**, *18*, 203–219. [CrossRef]
41. Wang, J.; Kwan, M.-P.; Xiu, G.; Deng, F. A robust method for evaluating the potentials of 15-minute cities: Implications for sustainable urban futures. *Geogr. Sustain*. **2024**, *5*, 597–606. [CrossRef]
42. Coutts, C. Greenway accessibility and physical-activity behavior. *Environ. Plan. B Plan. Des*. **2008**, *35*, 552–563. [CrossRef]
43. Vale, D.; Lopes, A.S. Accessibility inequality across Europe: A comparison of 15-minute pedestrian accessibility in cities with 100,000 or more inhabitants. *npj Urban Sustain*. **2023**, *3*, 55. [CrossRef]
44. Wali, B.; Frank, L.D.; Saelens, B.E.; Young, D.R.; Meenan, R.T.; Dickerson, J.F.; Keast, E.M.; Fortmann, S.P. Associations of walkability, regional and transit accessibility around home and workplace with active and sedentary travel. *J. Transp. Geogr.* **2024**, *116*, 103776. [CrossRef]
45. Nigg, C.; Alothman, S.A.; Alghannam, A.F.; Schipperijn, J.; AlAhmed, R.; Alsukait, R.F.; Rakic, S.; Cetinkaya, V.; Al-Hazzaa, H.M.; Alqahtani, S.A. A systematic review on the associations between the built environment and adult's physical activity in global tropical and subtropical climate regions. *Int. J. Behav. Nutr. Phys. Act*. **2024**, *21*, 59. [CrossRef]
46. Qiu, C.; Qiu, N.; Zhang, T. What causes the spatiotemporal disparities in greenway use intensity? Evidence from the central urban area of Beijing, China. *Front. Environ. Sci*. **2022**, *10*, 957641. [CrossRef]
47. He, D.; Lu, Y.; Xie, B.; Helbich, M. Large-scale greenway intervention promotes walking behaviors: A natural experiment in China. *Transp. Res. Part D Transp. Environ*. **2021**, *101*, 103095. [CrossRef]
48. Pontin, F.L.; Jenneson, V.L.; Morris, M.A.; Clarke, G.P.; Lomax, N.M. Objectively measuring the association between the built environment and physical activity: A systematic review and reporting framework. *Int. J. Behav. Nutr. Phys. Act*. **2022**, *19*, 119. [CrossRef]

Disclaimer/Publisher's Note: The statements, opinions and data contained in all publications are solely those of the individual author(s) and contributor(s) and not of MDPI and/or the editor(s). MDPI and/or the editor(s) disclaim responsibility for any injury to people or property resulting from any ideas, methods, instructions or products referred to in the content.